Integrated phase-change photonic devices and systems

C David Wright[1], Harish Bhaskaran[2] and Wolfram H P Pernice[3]

[1]Department of Engineering, University of Exeter, Exeter EX4 4QF, UK
[2]Department of Materials, University of Oxford, Oxford, OX1 3PH, UK
[3]Department of Physics, University of Münster, 48149 Münster, Germany

Abstract

Driven by the rapid rise of silicon-photonics, optical signalling is moving from the realm of long-distance communications to chip-chip and even on-chip domains. If on-chip signalling becomes optical, an obvious question to ask is whether we can do more than simply communicate with light. Can we, for example, store and process information directly in the optical domain? Can we supplement, or even surpass, the performance of electronic processors by exploiting the ultra-high bandwidth and wavelength division multiplexing capabilities offered by optics? In this article we show how, by using an integrated photonics platform that embeds chalcogenide phase-change materials into standard silicon photonics circuits, we might answer 'yes' to such questions. Specifically, we show that a phase-change integrated photonics platform can deliver binary and multilevel memory, arithmetic and logic processing, as well as synaptic and neuronal mimics for use in neuromorphic, or brain-like, computing - all working directly in the optical domain.

Keywords: memory, phase-transformation, nucleation & growth

Introduction

Optical fibers have, for several decades, carried most of our long-distance communications. This is because optical signaling combines ultra-high bandwidths, low losses and high energy efficiencies, to deliver an overall performance (for signal transmission) far superior to that available in the electrical domain. Short-haul optical signaling, especially for rack-to-rack connections in data centers, is also now commonplace. The next obvious step is to move to inter-chip, and even intra-chip, optical signaling. This could alleviate the bandwidth and power density limitations that currently act as bottlenecks to the performance of traditional semiconductor processing systems. This migration of optical signaling, from long-haul to on-chip applications, has benefited from rapid recent progress in silicon photonics that now offers a wide range of CMOS compatible integrated photonic components, including sources, detectors, modulators, switches, couplers etc.[1] Indeed, a single-chip processor that communicates directly with light has already been demonstrated[2].

If inter-chip and intra-chip signaling is likely to be light-based, it is pertinent to ask whether we should aim to carry out processing tasks, such as memory, arithmetic and logic, directly in the optical domain. Indeed, one might imagine the goal of realizing integrated photonic processors and memories that supplement, or in some applications replace, electronic implementations. How realistic is such a goal? One possible approach, that we discuss here, is by combining phase-change materials with standard silicon photonic devices and circuits. By this method it is possible to deliver photonic devices for non-volatile binary and multilevel memory, for arithmetic and logic processing, and for neuronal and synaptic hardware mimics. Moreover, these devices can be readily combined into larger-scale systems to provide, for example, all-optical non-von Neumann arithmetic and brain-like (neuromorphic) computing.

Device and system concepts

Binary and multilevel memory

Probably the simplest integrated phase-change photonic device is that for

the provision of memory. While previous promising approaches to the realization of integrated photonic memories have been reported[3-5], such devices were essentially inherently volatile. However, by combining chalcogenide phase-change materials with integrated photonics, we can achieve truly non-volatile storage, with stored states persevering for years, if not decades[6].

A schematic of the simplest integrated phase-change photonic memory device[7,8] is given in **Figure 1**a. Here, a small (micrometer or sub-micrometer sized) cell of phase-change material, here $Ge_2Sb_2Te_5$ (or GST) is deposited on top of a rib-type silicon (or silicon nitride) waveguide (a suitable encapsulation layer, ITO in Figure 1b, is also used to protect the phase-change material from oxidation). Since the refractive index of the amorphous and crystalline states of GST are very different[9-13] at the wavelengths (~ 1550 nm) used for silicon photonics, the waveguide's effective refractive index (see Figure 1b), and thus its optical attenuation, depends on the phase-state of the GST cell. This difference in optical attenuation forms the basis of the memory's *read* process; here a (low power) light pulse is sent along the waveguide and is attenuated to a greater or lesser degree, depending on whether the GST cell is crystalline or amorphous[7,8]. To switch the cell between states, i.e. to *write* and *erase* the cell, higher power light pulses are sent along the waveguide and, via optical coupling (Figure 1b), the GST cell is heated to the requisite temperatures for amorphization and crystallization, so realizing binary memory (Figure 1c). A pulsing scheme that is particularly efficacious for writing and erasing is shown in (the inset of) Figure 1d (and in Figure 1a). Here a rectangular (relatively) high power pulse is used to write an amorphous mark in the (previously fully crystalline) cell, while a double-step (dual-power) pulse is used to re-crystallize (erase) the cell. By controlling the amplitude and/or duration of the lower power section of the double-step pulse, the fraction of re-crystallized material can be closely controlled, leading to the realization of multilevel states (see Figure 1d)[14].

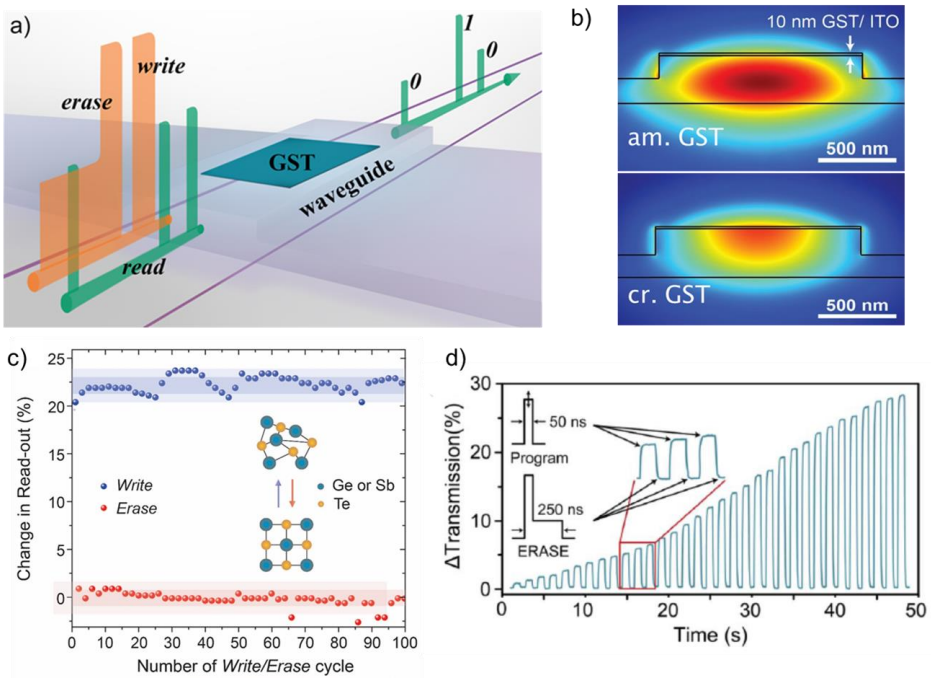

Figure 1. Integrated phase-change photonic device for binary and multilevel memory. (a) Schematic of device configuration. (b) Waveguide cross-section with simulated TE optical mode showing difference in coupling to (top) an amorphous and (bottom) a crystalline GST cell. (c) Repeated switching between crystalline and amorphous states, for binary memory operation. (d) Realization of multilevel states using a dual-step pulse approach (here 34 distinguishable states are achieved). [(b) and (c) adapted with permission from ref. 8; (c) from ref. 14].

In addition to using straight waveguides for the realization of memory, it also possible to use microring resonator structures, which are commonly used for photonics filters, modulators, switches and wavelength division multiplexing (WDM) applications[1,7,8,12]. For example, in **Figure 2**a we show a schematic of a WDM-enabled memory device (and in Figure 2b a fabricated device) in which three different wavelengths (here represented by red, green and blue, but in reality differing by less than 1 nm around 1550 nm) are selectively coupled to three microring resonators, each of which has its own integrated phase-change cell. In this arrangement, WDM can be used to selectively write, erase and read to each individual resonator, as shown experimentally in Figure 2c[8].

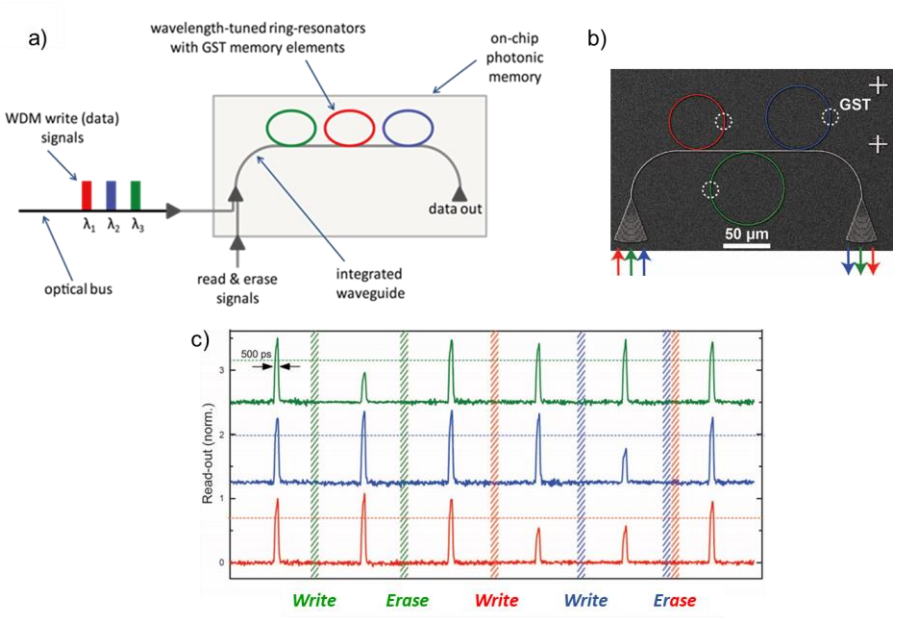

Figure 2. WDM-enabled all-optical memory. (a) Schematic of a WDM-enabled memory device. (b) Actual fabricated device of the type shown in (a). (c) Readout pulses from the device shown in (b), as the GST cell in each microring is selectively written and erased. [(b) and (c) adapted with permission from ref. 8].

Arithmetic processing

The ability to access multilevel states in the phase-change photonic cell means that we can do much more than simply store data. We can also carry out arithmetic processing, i.e. we can add, multiply, subtract and divide numbers. An example is shown in **Figure 3**a, here using a straight rib waveguide (of the kind shown in Figure 1a) to carry out the direct base-10 addition of 6 + 6. Initially, the phase-change cell is in the amorphous phase, which represents the number zero. Access to the multilevel states is obtained, in this case, by applying a sequence of (groups of) identical excitation pulses, each of which sets the cell to a pre-determined crystal fraction (so to a pre-determined waveguide transmission). For base-10 operation, the power and duration of the pulses is chosen such that it requires 10 (groups of) of them to fully re-crystallize the cell from its starting amorphous state[15]. Thus, to carry out addition of 6 + 6, six (groups of) pulses are sent into the waveguide, which sets the phase-change cell to level six. Then, the

second summand is added by sending in six more (groups of) pulses. When reaching the tenth level, the cell is reset to level zero, before the rest of the input sequence is applied. To register the carry-over of 10, a second phase-change cell is used to represent the 'tens', and this second cell is set to level 1 during the resetting (to zero) of the first cell. Thus, at the end of the calculation, the first cell representing the 'ones' is at level 2, while the second cell will be at level 1, revealing the expected answer of 12. The whole process can be thought of in terms of an analogy with an abacus[15], as also shown in Figure 3a.

The addition process above can also be used to implement multiplication (by successive addition), subtraction (by using the numbers complement approach to convert to addition) and division (successive subtraction). Moreover, by using multiple cells, with each cell representing successive powers of the base, we can easily represent very large or very small numbers. An important point to note also is that the result of the calculation is stored in the self-same device that carried out said calculation: processing and memory functions are thus merged, removing the well-known von Neumann bottleneck that plagues conventional computers.

Another arithmetic process that phase-change photonic devices are particularly well-suited to carrying out is that of matrix-vector multiplication. Matrix-vector (MV) multiplication is a key operation underpinning much of modern 'data science', from image processing to machine learning, data analytics etc. At the heart of MV operations is the scalar multiplication, $c = a \times b$. Rather than carrying out this multiplication using sequential addition as described in previous paragraphs, we can instead perform the multiplication directly using a single phase-change cell. We do this by coding the multiplier, a, into the transmission state of the cell (i.e. by setting the cell to a particular multilevel state) while the multiplicand, b, is coded into the (optical) power, P_{in}, of the readout pulse. The result of the multiplication, c, is thus calculated directly and appears as the power, P_{out}, of the readout signal (see Figure 3b)[16]. By using multiple cells and appropriate integrated photonic circuitry, it is relatively straightforward to extend this approach to deliver direct MV multiplication.

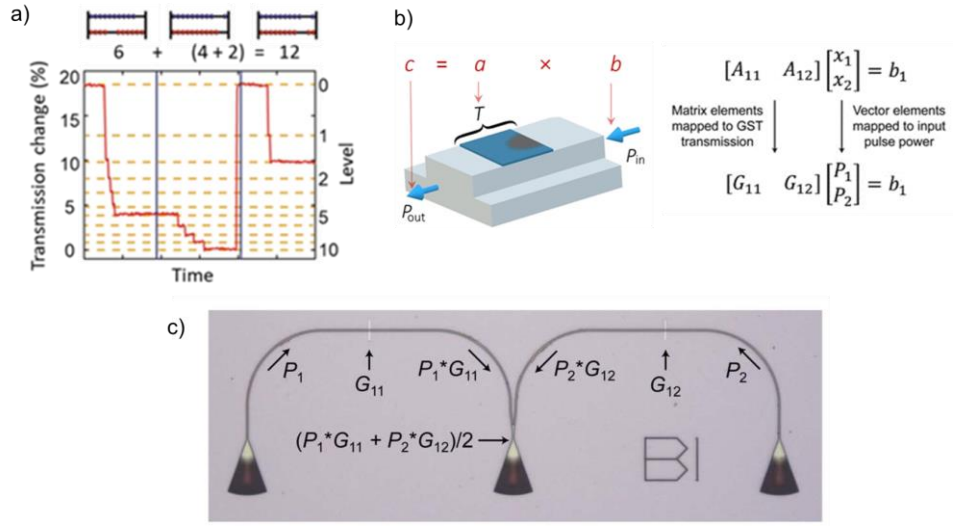

Figure 3. Arithmetic processing. (a) Direct addition of two base-10 numbers (using two photonic phase-change cells)[15] in a system analogous to the abacus. (b) Direct multiplication using a (left) single photonic phase-change and (right) extension to matrix-vector multiplication using multiple cells. (c) Experimental implementation of a [2×1] × [1×2] MV multiplier. [(a) adapted with permission from ref. 15; (b) and (c) from ref. 16].

An experimental implementation of the multiplication of a [2×1] matrix by a [1×2] vector is shown in Figure 3b. Scaling-up to larger MV operations is eminently possible, with suitable architectures. A major advantage of the use phase-change cells to store the matrix elements is that in applications where the same matrix elements are repeatedly used (e.g. in convolution-based processing), the programming of the matrix values needs to be done only once (since the cells are non-volatile), and thereafter the MV multiplication can be carried out extremely quickly indeed (using short, WDM optical pulses) and with very little energy budget. It should also be noted that the multilevel states of integrated photonic memories do not seem to suffer[16] from level drift that adversely affects electronic phase-change memories[17, 18].

Since we can carry out arithmetic using phase-change photonic devices, we can also carry out logic. Further details can be found in the literature[19].

Neuromorphic processing

As a final example of the potential of integrated phase-change photonics, we point out its ability to provide all-optical hardware mimics of brain synapses and neurons. A synapse can be thought of as providing a simple weighting operation between neurons. Thus, synaptic functionality can readily be provided by the straight rib waveguide device described above for use as a multilevel memory[20] (with the multilevel state mapped directly to the synaptic weight). At the system level, the outputs from multiple synapses can be combined (added) and input to a neuron using standard WDM techniques (see **Figure 4**).

To mimic the operation of a neuron, we can use a microring resonator with its own integrated phase-change cell that can be switched by the incoming combined pulses from all its synaptic connections[21,22]. Switching the neuronal cell in turn changes the optical resonance condition of the microring. Thus, in the scheme shown in Figure 4 (taken from Feldmann et al.[22]), when the neuronal cell is in the crystalline state, a probe pulse sent along the microring's 'output' waveguide couples strongly into the ring resonator and so no output pulse (neuronal spike) will be observed. However, if the instantaneous combined power of the pulses from all the synapses connected to the neuron is high enough to switch the neuronal cell to its amorphous state, the probe pulse is no longer on resonance with the microring and will be transmitted past the ring (i.e. the light pulse will mostly continue along the coupling 'output' waveguide), generating the neuron's output spike. Thus, the system naturally emulates the basic integrate-and-fire functionality of a biological neuron.

Combinations of synaptic and neuronal mimics of the type described above (see Figure 4b) have already been used to carry out the archetypal AI task of pattern recognition using both supervised and un-supervised learning[22].

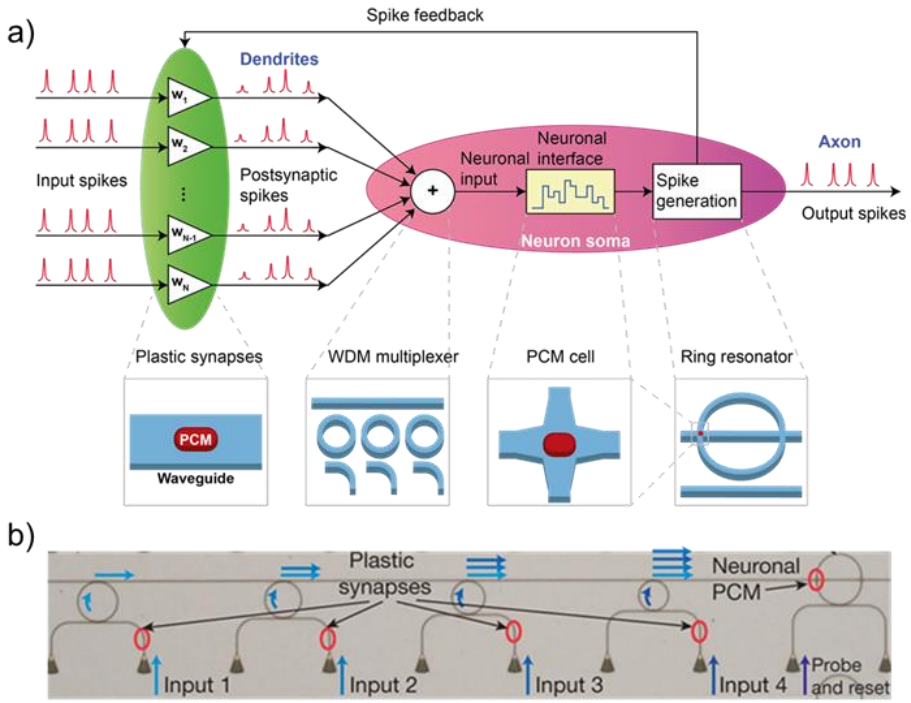

Figure 4. All-optical neuromorphic systems. (a) Schematic of the all-optical neuromorphic system implemented by Feldmann et al.[22] (top) and schematics of the constituent components (bottom) including (left to right) the synapses, multiplexer for summing outputs from all synapses and the phase-change (PCM) cell and microring resonator used to implement the neuron mimic. (b) A fabricated neuromorphic device, here with 4 synapses and a single neuron[22]. [(a) and (b) adapted with permission from ref. 22].

Summary and outlook

Integrated phase-change photonic devices and systems can clearly provide a wide range of all-optical memory and computing functionality. An advantage of using (chalcogenide) phase-change materials is their non-volatility. Written states are very stable (e.g. electronic phase-change memories have typical lifetimes of 10 years[6] at 80^0C), system power only being required when a state is changed (or read, but readout powers are low). The energy required for switching current phase-change photonic devices ranges from 50 pJ to a few nJ, depending on device architecture and size[8,14,23,24]. Methods by which switching energies could

be reduced are thus of much interest, with possible approaches already under development, such as via photonic crystal[25] or plasmonic waveguides[26]. By such means, and with the aid of further optimization, switching energies in the sub-pJ range should be feasible (switching energies of 0.1 pJ have already been achieved in electronic phase-change memories, with the potential for 20 aJ estimated[27]). Another area for potential improvement is switching speed. In many examples given in this article, excitation pulses were tens or hundreds of nanoseconds, though switching with (groups of) picosecond pulses has also been demonstrated[15]. The main limitations to speed are the finite crystallization time of phase-change materials, and the thermal time constant of the cell. Reducing the active volume of phase-change material is one way to improve on both these fronts. Tailoring of the excitation pulse, to ensure crystallization always occurs at the maximum rate, is another route to speed improvements[28]. A viable target in terms of minimum crystallization time is 0.5 ns (already achieved in both electronic[28] and optical[29] switching experiments), leading to GHz operation speeds. While GHz speeds are already achieved in electronics, a very significant advantage of optical processing is the ability to carry out many operations simultaneously using WDM techniques (as for example in the matrix-vector multiplication and neuromorphic processing examples above). Thus, operations that take many clock cycles in an electronic system could be carried out in the equivalent of a single clock cycle in the optical domain. Finally, we should mention the endurance of the phase-switching process, i.e. the number of times a cell may be switched between states. Electronic phase-change memories have demonstrated endurance potentially exceeding 10^{15} cycles[30], but higher figures may be needed for ultra-fast processing applications. Routes to this are most likely to come via materials development, perhaps by the so-called monatomic phase-change materials recently reported[31].

Acknowledgments

The authors acknowledge funding from the EU H2020 programme (grant #780848, Fun-COMP project). We would also like to thank the many members of

our research groups, and external collaborators, whose remarkable efforts generated much of the research results described in this article.

References

1. W. Bogaerts et al., *Laser Photonics Rev.* **6**, 47 (2012).

2. C. Sun et al., *Nature* **528**, 534 (2015).

3. K. Nozaki, A. Shinya, S. Matsuo, Y. Suzaki, T. Segawa, T. Sato, Y. Kawaguchi, R. Takahashi, M. Notomi, *Nat. Photonics* **6**, 248 (2012).

4. E. Kuramochi, K. Nozaki, A. Shinya, K. Takeda, T. Sato, S. Matsuo, H. Taniyama, H. Sumikura, Notomi, *Nat. Photonics* **8**, 474 (2014).

5. T. Alexoudi, D. Fitsios, A. Bazin, P. Monnier, R. Raj, A. Miliou, G. T. Kanellos, N. Pleros, F. Raineri, *IEEE J. Sel. Top. Quantum Electron*. **22**, 295 (2016).

6. A. Redaelli (editor), *Phase change memory: Device physics, reliability and applications* (Springer International Publishing AG, 2018).

7. C. Ríos, P. Hosseini, C.D. Wright, H. Bhaskaran, W.H.P. Pernice, *Adv. Mater*. **26** 1372 (2014).

8. C. Ríos, M. Stegmaier, P. Hosseini, D. Wang, T. Scherer, C.D. Wright, H. Bhaskaran and W.H.P. Pernice, *Nat. Photon.* **9**, 725 (2015).

9. K. Shportko S. Kremers, M. Woda, D. Lencer, J. Robertson, M. Wuttig. *Nat. Mater.* **7**, 653 (2008).

10. W.H.P. Pernice , H. Bhaskaran, App. Phys. Lett. 101, 171101(2012)

11. B. Gholipour et al., *Adv. Mater.* 25, 3050 (2013).

12. M. Rude , J. Pello , R. E. Simpson , J. Osmond , G. Roelkens , J.J.G.M. van der Tol, V. Pruneri , *Appl. Phys. Lett.* **103**, 141119 (2013).

13. C. R. de Galarreta, A. M. Alexeev, Y-Y. Au, M. Lopez-Garcia, M. Klemm, M. Cryan, J. Bertolotti and C.D. Wright, *Adv. Funct. Mater.* **28,** 1704993 (2018)

14. X. Li, N. Youngblood, C. Ríos, Z. Cheng, C. D. Wright, W.H.P. Pernice and H. Bhaskaran, *Optica* **6**, 1 (2019).

15. J. Feldmann, M. Stegmaier, N. Gruhler, C. Ríos, H. Bhaskaran H, C.D. Wright, W.H.P. Pernice, *Nature Comms* **8**, 1256 (2017).

16. C. Ríos, N. Youngblood, Z. Cheng, M. Le Gallo, W.H.P. Pernice, C.D. Wright, A. Sebastian, H. Bhaskaran, *Sci. Adv.* **5**, 5759 (2019).

17. I. V. Karpov, M. Mitra, D. Kau, G. Spadini, Y. A. Kryukov, V. G. Karpov, *J. Appl. Phys.* **102**, 124503 (2007).

18. P. Fantini, S. Brazzelli, E. Cazzini, A. Mani, *Appl. Phys. Lett.* **100**, 013505 (2012).

19. Z. Cheng, C. Ríos, N. Youngblood, C.D.Wright, W.H.P. Pernice. H. Bhaskaran, *Adv. Mater.* **30**, 1802435 (2018).

20. Z. Cheng, C. Ríos, W.H.P. Pernice, C.D. Wright. H. Bhaskaran, *Sci. Adv.* **3**, e1700160 (2017).

21. I. Chakraborty, G. Saha, A. Sengupta, K. Roy, *Sci.Rep.* 8, 12980 (2018)

22. J. Feldmann, N. Youngblood, C.D. Wright, H. Bhaskaran and W.H.P. Pernice, *Nature* **569**, 208 (2019).

23. M. Stegmaier, C. Ríos, H. Bhaskaran, C.D. Wright, W.H P. Pernice, *Adv. Opt. Mater.* **5**, 1600346 (2017).

24. C. Wu, H. Yu, H. Li, X. Zhang, I. Takeuchi, M. Li, *ACS Photonics* **6**, 87 (2019).

25. J. Von Keitz, J. Feldmann, N. Gruhler, C. Ríos, C.D. Wright, H. Bhaskaran, W.H.P. Pernice WHP. *ACS Photonics* **5**, 4644 (2018).

26. N. Farmakidis, N. Youngblood, X. Li, J. Tan, J.L. Swett, Z. Cheng, C. David Wright, W.H.P. Pernice, H. Bhaskaran, *Sci. Adv.*, in press (2019)

27. F. Xiong, A.D. Liao, D. Estrada, E. Pop, Science **332**, 568 (2011)

28. D. Loke, T. H. Lee2, W.J. Wang, L.P. Shi, R. Zhao, Y.C. Yeo, T.C. Chong, S. R. Elliott, Science **336**, 1566 (2012).

29. J. Siegel, C.N. Afonso, J. Solis, *Appl. Phys. Lett.* **75**, 3102 (1999).

30. I. S. Kim et al., *IEEE Symp. VLSI Technol*. IEEE, Honolulu, HI, USA, pp. 203 (2010).

31. M. Salinga et al., *Nature Mater.* **17**, 681 (2018).